Membrane Proteins

Deutsche Ausgabe: DOI: 10.1002/ange.201509910
Internationale Ausgabe: DOI: 10.1002/anie.201509910

Monitoring Backbone Hydrogen-Bond Formation in β-Barrel Membrane Protein Folding

*Thomas Raschle, Perla Rios Flores, Christian Opitz, Daniel J. Müller, and Sebastian Hiller**

Abstract: *β-barrel membrane proteins are key components of the outer membrane of bacteria, mitochondria and chloroplasts. Their three-dimensional structure is defined by a network of backbone hydrogen bonds between adjacent β-strands. Here, we employ hydrogen–deuterium (H/D) exchange in combination with NMR spectroscopy and mass spectrometry to monitor backbone hydrogen bond formation during folding of the outer membrane protein X (OmpX) from E. coli in detergent micelles. Residue-specific kinetics of interstrand hydrogen-bond formation were found to be uniform in the entire β-barrel and synchronized to formation of the tertiary structure. OmpX folding thus propagates via a long-lived conformational ensemble state in which all backbone amide protons exchange with the solvent and engage in hydrogen bonds only transiently. Stable formation of the entire OmpX hydrogen bond network occurs downhill of the rate-limiting transition state and thus appears cooperative on the overall folding time scale.*

Integral β-barrel membrane proteins are the predominant structural class in the outer membranes of bacteria, chloroplasts and mitochondria.[1–4] The three-dimensional structure of a β-barrel membrane protein is defined by backbone hydrogen bonds between adjacent strands.[2,5,6] The biogenesis pathways of β-barrel membrane proteins are essential, but the underlying mechanism is still unclear.[7–9] In vitro, β-barrel membrane proteins can be functionally refolded from a chaotrope-denatured state into detergent micelles or lipid bilayers, ending up in their native structure.[10–12] Atomic resolution descriptions of in vitro folding thus provide important benchmark data for the folding biophysics and yield insight into structural determinants. In vitro folding of β-barrel membrane proteins has been characterized using biophysical and biochemical methods, including fluorescence spectroscopy,[13,14] circular dichroism (CD) spectroscopy,[15–17] SDS-PAGE migration shifts,[18,19] and single-molecule force spectroscopy.[20] However, despite the fundamental role for the protein structure, the formation of the hydrogen bond network during β-barrel membrane protein folding has so far not been observed at the atomic level.

Here, we monitor the formation of interstrand hydrogen bonds during the folding process of a β-barrel membrane protein in detergent micelles by hydrogen–deuterium (H/D) exchange in combination with NMR spectroscopy and mass spectrometry.[21,22] We use the 8-stranded OmpX from *E. coli* as a model system.[23,24] At the onset of the experiment, OmpX (148 aa) is solubilized in chaotropic denaturant solution, where the polypeptide is fully unfolded and adopts a random coil conformation without residual structure.[25–27] Using a manually operated, custom-built setup (Figure S1 in the Supporting Information), folding is triggered by rapid dilution with an aqueous folding buffer that contains the detergent micelles. This initial rapid dilution step is performed in deuterated solvent, leading to the incorporation of deuterons at all exchange-accessible backbone amide positions. The sample is then incubated for a variable folding time *T*, after which a second rapid dilution step with hydrogen-based folding buffer is performed, reducing the deuterium content in the solvent by about 80% (Figure S1). Finally, the sample is incubated until protein folding has progressed to completion.

Folded OmpX in detergent micelles of dodecylphosphocholine (DPC) or lauryldimethylamine-*N*-oxide (LDAO) features a well-dispersed NMR spectrum, allowing sequence-specific quantification of deuterium incorporation levels as a function of the folding time *T* by peak volume integration (Figure 1A). Amide protons in the loops and turns of OmpX rapidly exchange with the solvent, resulting in their full protonation irrespective of the folding time *T*. An example is given by residue G16 in the first extracellular loop, which has constant intensity (Figure 1B). On the other hand, backbone amide protons that are involved in stable hydrogen bonds at the time *T* and until completion of the folding process, show a time-dependent intensity decrease towards the level of residual hydrogen in the folding buffer. Examples are given by residues V83, G86 or V144 (Figure 1B).

For β-barrel membrane proteins, the observation of hydrogen bond formation kinetics by H/D-exchange in our experiment requires two conditions, namely that 1) protein folding kinetics are substantially slower than amide proton exchange kinetics for unprotected amide moieties and 2) that in the folded protein amide proton exchange is slow relative to the time required to experimentally quantify the deuterium incorporation levels. Both these conditions are fulfilled for OmpX, since 1) unprotected amide protons have an intrinsic solvent exchange rate $k_{ex} > 20\ s^{-1}$ at the experimental pH of 7.9,[28] about three orders of magnitude faster than the global folding kinetics, and since 2) backbone amide protons in the

[*] Dr. T. Raschle, P. Rios Flores, C. Opitz, Prof. Dr. S. Hiller
Biozentrum, University of Basel
Klingelbergstrasse 70, 4056 Basel (Switzerland)
E-mail: sebastian.hiller@unibas.ch
P. Rios Flores, Prof. Dr. D. J. Müller
Department of Biosystems Science and Engineering
Eidgenössische Technische Hochschule Zürich
Mattenstrasse 26, 4058 Basel (Switzerland)

Supporting information (details on protein biochemistry, fluorescence spectroscopy, NMR spectroscopy and mass spectrometry) and the ORCID identification number(s) for the author(s) of this article can be found under http://dx.doi.org/10.1002/anie.201509910.

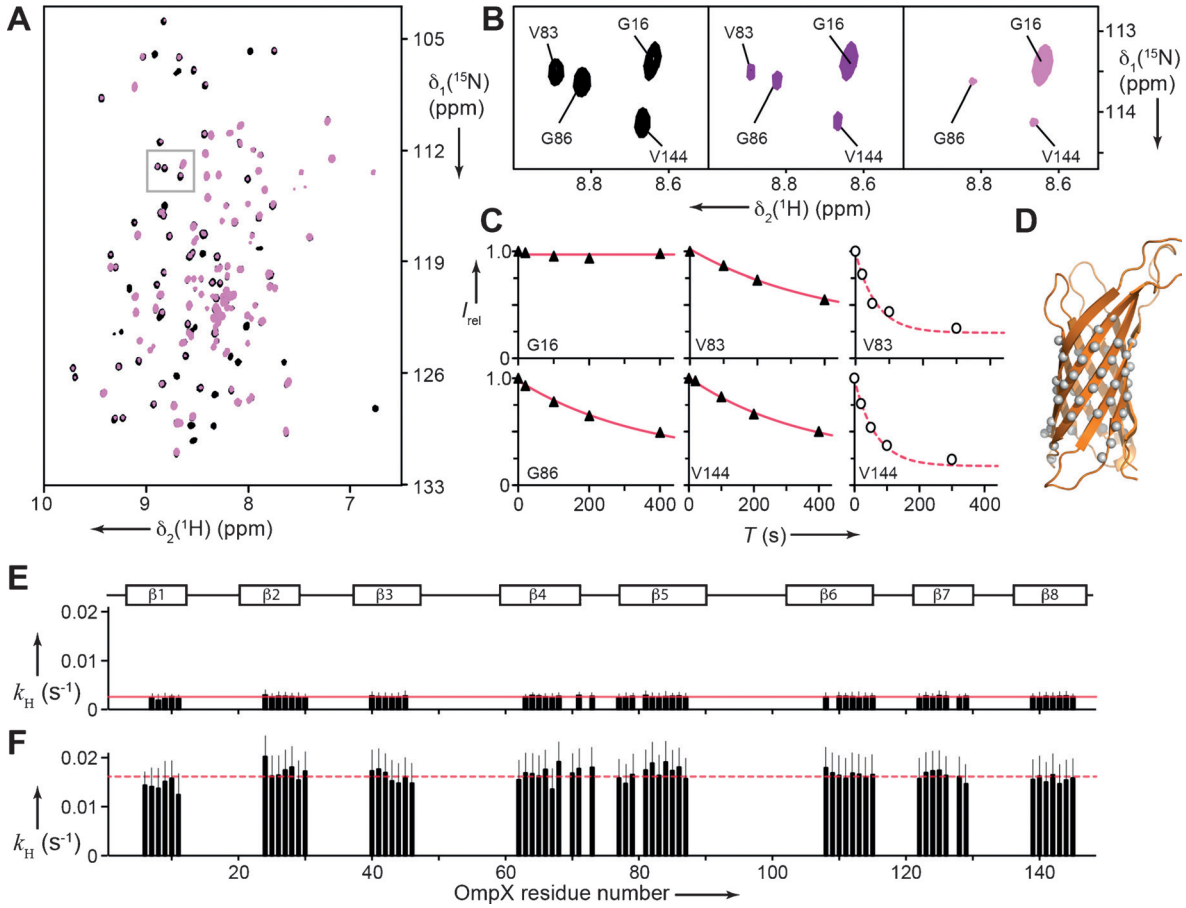

Figure 1. Residue-specific hydrogen bond formation kinetics of OmpX as monitored by high-resolution NMR spectroscopy in combination with H/D-exchange. A) 2D [^{15}N,^{1}H]-TROSY spectra of OmpX in DPC micelles. Black: Spectrum after folding in H_2O-based buffer. Magenta: Spectrum after folding in D_2O-based buffer with a folding time $T = 400$ s. A black peak is present below each magenta peak. Peak intensities vary due to the differential incorporation of deuterium at the backbone amide position. B) Enlargement of a spectral section (outlined grey in A), with four resonances at different folding times T. Black: $T = 0$ s, purple: $T = 100$ s, magenta: $T = 400$ s. C) Relative NMR signal intensity, I_{rel}, as a function of the folding time T for the amino acid residues shown in (B). The experimental data (symbols) have been fitted to single exponentials (red lines). Black triangles and solid lines: Folding into DPC detergent; White circles and dashed lines: Folding into LDAO detergent. Error bars from spectral noise are smaller than the symbols. D) NMR solution structure of OmpX in ribbon representation (PDB 1Q9F).[23] All backbone amide protons with half life time constants >100 h are indicated as white spheres. E,F) Residue-specific hydrogen bond formation rate constants $k_H(i)$ for OmpX folding into (E) DPC detergent and (F) LDAO detergent. The horizontal lines indicate the average values $\langle k_H(i)\rangle$. The secondary structure of folded OmpX with eight β-strands β1–β8 is indicated.

strands of the folded OmpX β-barrel are protected by hydrogen bonds with exchange rate constants consistently smaller than $k_{ex} < 3 \times 10^{-6}\ s^{-1}$ (lifetimes larger than 100 h, Figure S2A). For OmpX, the well-protected residues comprise residues 6–11, 24–30, 40–47, 62–67, 70, 71, 73, 77–87, 108–115, 122–126, 128, 129, 137, and 139–148 in the eight β-strands (Figure 1D). For these residues, hydrogen bond formation kinetics were reliably obtained.

The deuterium incorporation as a function of the folding time T was found to be well described by single exponentials, yielding for each residue i the specific hydrogen bond formation rate constant $k_H(i)$ (Figure 1C). For OmpX refolding into DPC micelles, these constants were found to be identical within experimental error along the amino acid sequence with an average value of $\langle k_H(i)\rangle = 0.0026\ s^{-1}$ (Figure 1E). Equivalent experiments with the alternative detergent LDAO showed also uniform sequence-specific hydrogen bond formation kinetics with an average rate constant of $\langle k_H(i)\rangle = 0.016\ s^{-1}$, that is, about one order of magnitude faster than in DPC (Figure 1F).

Because the residue-specific hydrogen bond formation rate constants do not resolve correlations between amide moieties on individual OmpX molecules, they are compatible with different scenarios for the folding mechanism, in which folding may or may not proceed through intermediate states with stable secondary structure. In the present system, two fundamentally different types of mechanism can be assumed, which both would give rise to the observed residue-specific hydrogen bond formation kinetics (Figure S3). In mechanism type I, formation of the 8-stranded β-sheet is a slow, rate-limiting step and subsequent circular closure of the barrel is a fast reaction. In mechanism type II, multiple conformations with the β-sheet formed to different extent stand in fast equilibrium and the final circular closure of the barrel is the

rate-limiting step. Mass spectrometry provides an experimental way to distinguish between these scenarios that can not be resolved by NMR spectroscopy alone, as previously highlighted by Miranker et al.[29] We thus employed mass spectrometric analysis of H/D-exchanged samples to address the existence of folding intermediates and thus to distinguish between these scenarios (Figure 2). Fully protonated OmpX

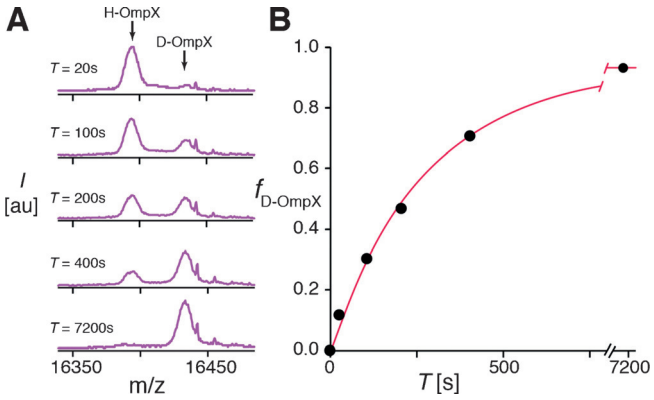

Figure 2. Hydrogen bond formation kinetics of individual OmpX molecules as monitored by mass spectrometry (MS) in combination with H/D-exchange. A) MS spectra of OmpX folding into DPC detergent micelles at different folding times *T*, as indicated. The arrows indicate the positions of the protonated and deuterated species of OmpX (H-OmpX and D-OmpX, respectively). B) Fraction of the deuterated species, $f_{\text{D-OmpX}}$, as a function of the refolding time *T*. The experimental data (black dots) was fitted with a single exponential (red line), yielding a folding rate constant of $k_F = 0.0032\ s^{-1}$.

was observed at a molecular mass of 16394 Da, whereas OmpX with fully deuterated barrel features a mass of 16434 Da. Sampling of the folding time revealed a bimodal population shift from the protonated to the deuterated molecule, without significantly populated intermediate species, thus identifying type II as the mechanism underlying OmpX folding. Stable formation of the entire hydrogen bond network of OmpX thus appears as a cooperative event, following a single exponential function with a global hydrogen bond network formation rate constant of $k_H = 0.0032\ s^{-1}$. This constant coincides within experimental error with the average rate constant of residue-specific hydrogen bond formation $\langle k_H(i) \rangle$ (Table 1).

Finally, to correlate the hydrogen bond formation kinetics to the overall protein folding process, time-resolved fluorescence spectroscopy monitoring tryptophan residues was employed. OmpX contains two natural tryptophan residues, W76 and W140, located in a periplasmic turn T2, and in strand 8, respectively (Figure S4). Folded and unfolded OmpX have different fluorescence emission spectra, and the time-dependent changes at fixed wavelength thus suitably monitor the unfolding-folding transition.[30–32] We monitored the time-dependence of the fluorescence emission under equivalent biochemical conditions as in the H/D-exchange experiments, that is, triggered by rapid dilution of a chaotrope-denatured state with aqueous buffer in a ratio of 1:10. The folding kinetics follow a two-state folding model with a single exponential rate constant (Figure S5). For OmpX folding into DPC detergent, the observed protein folding rate constant of $k_F = 0.0027\ s^{-1}$ corresponds within experimental error to the average hydrogen-bond formation kinetic rate constant of $\langle k_H(i) \rangle$ and the global hydrogen bond network formation constant k_H (Table 1). A set of corresponding rate constants was also found for OmpX folding in the detergent LDAO, in magnitude about one order larger than folding in DPC (Table 1).

Overall, folding of the β-barrel protein OmpX in detergent micelles thus follows a 2-state mechanism of type II (Figure 3). Initially, upon rapid dilution of the denatured protein, the unfolded polypeptide chain undergoes a hydrophobic collapse and associates with detergent molecules forming a mixed micelle. These initial reaction steps occur on the order of a few microseconds[33] and are not resolved in the H/D-exchange setup or by real-time fluorescence spectroscopy. The resulting state is a conformational ensemble in which the OmpX polypeptide chain interconverts between different short-lived, partially folded conformations (Figure 3).

By this permanent structural rearrangement, long-term stable hydrogen bonds are not formed and all amide moieties

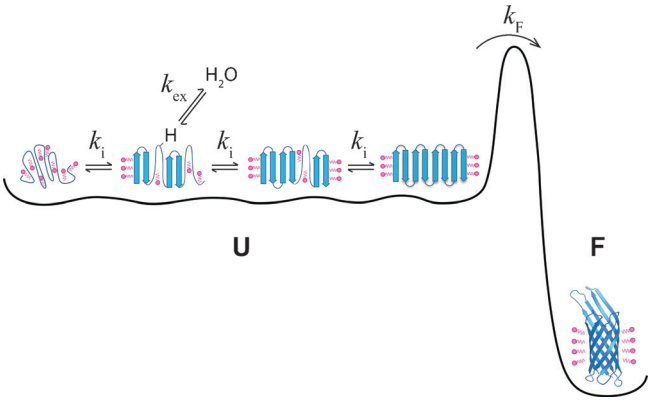

Figure 3. Free energy diagram for OmpX folding into detergent micelles. Upon rapid dilution from a denatured state, OmpX associates with detergent micelles to a dynamic conformational ensemble state (U). Four arbitrary conformations are shown in cartoon representation, as representatives for the dynamic ensemble. In this state, multiple conformations rapidly interconvert with kinetic rate constants k_i. No long-lived hydrogen bonds are formed, so that all backbone amides are effectively accessible to chemical exchange (k_{ex}) with the solvent. The folded state of OmpX (F) is separated from the conformational ensemble by a rate-limiting folding step with a kinetic rate constant k_F on the minutes time scale (Table 1).

Table 1: Rate constants of OmpX folding as a function of folding conditions.

Detergent	$\langle k_H(i) \rangle$ [s^{-1}][a]	k_H [s^{-1}][b]	k_F [s^{-1}][c]
DPC	0.0026 ± 0.0002	0.0032 ± 0.0007	0.0027 ± 0.0001
LDAO	0.016 ± 0.002	0.018 ± 0.008	0.015 ± 0.001

[a] Average residue-specific hydrogen bond formation rate constant, determined by NMR spectroscopy. [b] Global hydrogen bond formation rate constant, determined by mass-spectrometry. [c] Protein folding rate constant, determined by real-time tryptophan fluorescence spectroscopy.

along the polypeptide chain are accessible to exchange with the solvent. Any possible intermediates, such as partially or fully formed β-sheets, are dynamically unstable. Subsequent formation of the three-dimensional barrel structure is an irreversible process, driven by the thermodynamic stability of the folded protein. The rate-limitation of the reaction is likely imposed by the conformational search of the polypeptide chain for circular closure, and the statistically low likelihood of this event compared to other conformational rearrangements.[34] Furthermore, whereas the detergent chemistry can modulate the magnitude of the rates (Table 1), the mechanism of cooperative, global formation of the hydrogen bond network is preserved in different detergents.

In summary, we have demonstrated the application of H/D-exchange experiments for the determination of hydrogen bond formation kinetics during folding of a β-barrel membrane protein into detergent micelles. Residue-specific kinetics of interstrand hydrogen-bond formation were found to be uniform along the amino acid sequence and synchronized to the formation of the protein tertiary structure. The H/D-exchange setup is compatible with membrane mimetics other than detergents, including bicelles, liposomes, and lipid bilayer nanodiscs, as well as with other β-barrel membrane proteins, and it is also capable to detect partially folded intermediates. Its application will thus be of special interest in situations, where sequence-dependent intermediates may be expected, such as insertase-assisted folding of outer membrane proteins into lipid bilayers.[7–9]

Acknowledgements

This work was supported by grants from the Swiss National Science Foundation (Grant PP00P3_128419) and the European Research Council (FP7 contract MOMP 281764) to S.H. and by the Swiss Nanoscience Institute to S.H. and D.J.M.

Keywords: fluorescence spectroscopy · mass spectrometry · membrane proteins · NMR spectroscopy · protein folding

How to cite: *Angew. Chem. Int. Ed.* **2016**, *55*, 5952–5955
Angew. Chem. **2016**, *128*, 6056–6059

[1] K. P. Locher, B. Rees, R. Koebnik, A. Mitschler, L. Moulinier, J. P. Rosenbusch, D. Moras, *Cell* **1998**, *95*, 771–778.
[2] G. E. Schulz, *Curr. Opin. Struct. Biol.* **2000**, *10*, 443–447.
[3] N. Pfanner, N. Wiedemann, C. Meisinger, T. Lithgow, *Nat. Struct. Mol. Biol.* **2004**, *11*, 1044–1048.
[4] S. Hiller, R. G. Garces, T. J. Malia, V. Y. Orekhov, M. Colombini, G. Wagner, *Science* **2008**, *321*, 1206–1210.
[5] S. Hiller, G. Wagner, *Curr. Opin. Struct. Biol.* **2009**, *19*, 396–401.
[6] J. W. Fairman, N. Noinaj, S. K. Buchanan, *Curr. Opin. Struct. Biol.* **2011**, *21*, 523–531.
[7] N. Noinaj, A. J. Kuszak, J. C. Gumbart, P. Lukacik, H. Chang, N. C. Easley, T. Lithgow, S. K. Buchanan, *Nature* **2013**, *501*, 385–390.
[8] F. Gruss, F. Zähringer, R. P. Jakob, B. M. Burmann, S. Hiller, T. Maier, *Nat. Struct. Mol. Biol.* **2013**, *20*, 1318–1320.
[9] C. L. Hagan, T. J. Silhavy, D. Kahne, *Annu. Rev. Biochem.* **2011**, *80*, 189–210.
[10] S. K. Buchanan, *Curr. Opin. Struct. Biol.* **1999**, *9*, 455–461.
[11] S. K. Buchanan, B. S. Smith, L. Venkatramani, D. Xia, L. Esser, M. Palnitkar, R. Chakraborty, D. van der Helm, J. Deisenhofer, *Nat. Struct. Biol.* **1999**, *6*, 56–63.
[12] S. Hiller, J. Abramson, C. Mannella, G. Wagner, K. Zeth, *Trends Biochem. Sci.* **2010**, *35*, 514–521.
[13] T. Surrey, A. Schmid, F. Jähnig, *Biochemistry* **1996**, *35*, 2283–2288.
[14] J. H. Kleinschmidt, L. K. Tamm, *Biochemistry* **1999**, *38*, 4996–5005.
[15] J. H. Kleinschmidt, L. K. Tamm, *J. Mol. Biol.* **2002**, *324*, 319–330.
[16] D. Chaturvedi, R. Mahalakshmi, *PLoS One* **2013**, *8*, e79351.
[17] S. R. Maurya, D. Chaturvedi, R. Mahalakshmi, *Sci. Rep.* **2013**, *3*, 1989.
[18] J. H. Kleinschmidt, M. C. Wiener, L. K. Tamm, *Protein Sci.* **1999**, *8*, 2065–2071.
[19] D. Gessmann, Y. H. Chung, E. J. Danoff, A. M. Plummer, C. W. Sandlin, N. R. Zaccai, K. G. Fleming, *Proc. Natl. Acad. Sci. USA* **2014**, *111*, 5878–5883.
[20] M. Damaghi, S. Köster, C. A. Bippes, O. Yildiz, D. J. Müller, *Angew. Chem. Int. Ed.* **2011**, *50*, 7422–7424; *Angew. Chem.* **2011**, *123*, 7560–7562.
[21] H. Roder, K. Wüthrich, *Proteins Struct. Funct. Genet.* **1986**, *1*, 34–42.
[22] S. E. Radford, C. M. Dobson, P. A. Evans, *Nature* **1992**, *358*, 302–307.
[23] C. Fernández, C. Hilty, G. Wider, P. Güntert, K. Wüthrich, *J. Mol. Biol.* **2004**, *336*, 1211–1221.
[24] J. Vogt, G. E. Schulz, *Structure* **1999**, *7*, 1301–1309.
[25] S. Hiller, G. Wider, L. L. Imbach, K. Wüthrich, *Angew. Chem. Int. Ed.* **2008**, *47*, 977–981; *Angew. Chem.* **2008**, *120*, 992–996.
[26] H. Tafer, S. Hiller, C. Hilty, C. Fernández, K. Wüthrich, *Biochemistry* **2004**, *43*, 860–869.
[27] V. Kräutler, S. Hiller, P. H. Hünenberger, *Eur. Biophys. J.* **2010**, *39*, 1421–1432.
[28] K. Wüthrich, *NMR of Proteins and Nucleic Acids*, Wiley, New York, **1986**.
[29] A. Miranker, C. V. Robinson, S. E. Radford, R. T. Aplin, C. M. Dobson, *Science* **1993**, *262*, 896–900.
[30] J. H. Kleinschmidt, L. K. Tamm, *Biochemistry* **1996**, *35*, 12993–13000.
[31] T. Surrey, F. Jähnig, *J. Biol. Chem.* **1995**, *270*, 28199–28203.
[32] L. M. McMorran, A. I. Bartlett, G. H. Huysmans, S. E. Radford, D. J. Brockwell, *J. Mol. Biol.* **2013**, *425*, 3178–3191.
[33] P. J. Bond, J. Cuthbertson, M. S. Sansom, *Biochem. Soc. Trans.* **2005**, *33*, 910–912.
[34] K. W. Plaxco, K. T. Simons, I. Ruczinski, D. Baker, *Biochemistry* **2000**, *39*, 11177–11183.

Received: October 23, 2015
Revised: December 16, 2016
Published online: April 9, 2016

